REPORT DOCUMENTATION PAGE	Form Approved OMB NO. 0704-0188

1. REPORT DATE (DD-MM-YYYY)	2. REPORT TYPE	3. DATES COVERED (From - To)
15-08-2013	Book	-

4. TITLE AND SUBTITLE
InAs1-xSbx alloys with native lattice parameters grown on compositionally graded buffers: structural and optical properties

5a. CONTRACT NUMBER
W911NF-12-2-0057

5b. GRANT NUMBER

5c. PROGRAM ELEMENT NUMBER
611102

5d. PROJECT NUMBER

5e. TASK NUMBER

5f. WORK UNIT NUMBER

6. AUTHORS
Ding Wang, Dmitry Donetsky, Youxi Lin, Gela Kipshidze, Leon Shterengas, Gregory Belenky, Wendy L. Sarney, Stefan P. Svensson

7. PERFORMING ORGANIZATION NAMES AND ADDRESSES
Research Foundation of SUNY at Stony Brook U
Office of Sponsored Programs
W-5510 Melville Library
Stony Brook, NY 11794 -3362

8. PERFORMING ORGANIZATION REPORT NUMBER

9. SPONSORING/MONITORING AGENCY NAME(S) AND ADDRESS(ES)
U.S. Army Research Office
P.O. Box 12211
Research Triangle Park, NC 27709-2211

10. SPONSOR/MONITOR'S ACRONYM(S)
ARO

11. SPONSOR/MONITOR'S REPORT NUMBER(S)
62447-EL.3

12. DISTRIBUTION AVAILIBILITY STATEMENT
Approved for public release; distribution is unlimited.

13. SUPPLEMENTARY NOTES
The views, opinions and/or findings contained in this report are those of the author(s) and should not contrued as an official Department of the Army position, policy or decision, unless so designated by other documentation.

14. ABSTRACT
GaInSb and AlGaInSb compositionally graded buffer layers grown on GaSb by MBE were used to develop unrelaxed InAs1-xSbx epitaxial alloys with strain-free native lattice constants up to 2.1% larger than that of GaSb. The in-plane lattice constant of the strained to buffer layer was grown to be equal to the native, unstrained lattice constant of InAs1-xSbx with given x. The InAs0.56As0.44 layers demonstrated a photoluminescence (PL) peak at 9.4 um at T=150K. The minority carrier lifetime measured at 77K for InAs0.8Sb0.2 was 250 ns.

15. SUBJECT TERMS
InAsSb, compositionally graded buffer, MBE, infrared, minority carrier lifetime, reciprocal space mapping

16. SECURITY CLASSIFICATION OF:			17. LIMITATION OF ABSTRACT	15. NUMBER OF PAGES	19a. NAME OF RESPONSIBLE PERSON
a. REPORT	b. ABSTRACT	c. THIS PAGE			Gregory Belenky
UU	UU	UU	UU		19b. TELEPHONE NUMBER 631-632-8397

Report Title

InAs1-xSbx alloys with native lattice parameters grown on compositionally graded buffers: structural and optical properties

ABSTRACT

GaInSb and AlGaInSb compositionally graded buffer layers grown on GaSb by MBE were used to develop unrelaxed InAs1-xSbx epitaxial alloys with strain-free native lattice constants up to 2.1% larger than that of GaSb. The in-plane lattice constant of the strained to buffer layer was grown to be equal to the native, unstrained lattice constant of InAs1-xSbx with given x. The InAs0.56As0.44 layers demonstrated a photoluminescence (PL) peak at 9.4 um at T=150K. The minority carrier lifetime measured at 77K for InAs0.8Sb0.2 was 250 ns.

ure Force

vanced

ications

Frontier
al Defense

nical,

11

e found at

Selected Topics in Electronics and Systems – Vol. 53

FRONTIERS IN ELECTRONICS

Selected Papers from the Workshop on Frontiers in Electronics 2011 (WOFE-11)

San Juan, Puerto-Rico 18 – 21 December 2011

Editors

Sorin Cristoloveanu
IMEP, INP Grenoble – MINATEC, France

Michael S. Shur
Rensselaer Polytechnic Institute, USA

World Scientific

NEW JERSEY • LONDON • SINGAPORE • BEIJING • SHANGHAI • HONG KONG • TAIPEI • CHENNAI

Published by

World Scientific Publishing Co. Pte. Ltd.

5 Toh Tuck Link, Singapore 596224

USA office: 27 Warren Street, Suite 401-402, Hackensack, NJ 07601

UK office: 57 Shelton Street, Covent Garden, London WC2H 9HE

British Library Cataloguing-in-Publication Data
A catalogue record for this book is available from the British Library.

Selected Topics in Electronics and Systems — Vol. 53
FRONTIERS IN ELECTRONICS
Selected Papers from the Workshop on Frontiers in Electronics 2011 (WOFE-11)

ISBN 978-981-4536-84-4

Printed in Singapore

The seventh in tl
took place in San

went to E. Ca
F. Barbagini, E.
"Efficient phosph
nanocolumnar LE
Hwang, Eun Jeor
Chun Hum Cho
of Metal/PVDF-tr
place in the Best I
paper "Carbon Na
and Management
their paper entitlec
Semiconductor," r
This issue inc
selected after the

, M. Stanacevic, A. V.
eles, W. K. Chan, and Z.
on of InP scintillation,"
sited," *IEEE J. Selected*
l Journal of High Speed
ı-proportionality," *IEEE*

$InAs_{1-x}Sb_x$ ALLOYS WITH NATIVE LATTICE PARAMETERS GROWN ON COMPOSITIONALLY GRADED BUFFERS: STRUCTURAL AND OPTICAL PROPERTIES

D. WANG, D. DONETSKY, Y. LIN, G. KIPSHIDZE, L. SHTERENGAS and G. BELENKY*

Department of ECE, Stony Brook University, Stony Brook, New York 11794
**garik@ece.sunysb.edu*

W. L. SARNEY and S. P. SVENSSON

U.S. Army Research Laboratory, 2800 Powder Mill Rd, Adelphi, Maryland 20783

GaInSb and AlGaInSb compositionally graded buffer layers grown on GaSb by MBE were used to develop unrelaxed $InAs_{1-x}Sb_x$ epitaxial alloys with strain-free native lattice constants up to 2.1% larger than that of GaSb. The in-plane lattice constant of the strained top buffer layer was grown to be equal to the native, unstrained lattice constant of $InAs_{1-x}Sb_x$ with given x. The $InAs_{0.56}Sb_{0.44}$ layers demonstrated a photoluminescence (PL) peak at 9.4 μm at T = 150 K. The minority carrier lifetime measured at 77 K for $InAs_{0.8}Sb_{0.2}$ was 250 ns.

Keywords: InAsSb; compositionally graded buffer; MBE; infrared, minority carrier lifetime; reciprocal space mapping.

Introduction

GaSb based III-V materials are widely used in the development of mid- and long-wave infrared optoelectronic devices because of the narrow bandgap and the flexibility in forming heterojunctions with various types of band offsets, i.e. type I, type II staggered or type II broken gap. For device applications, heterostructures with a considerable thickness are preferably grown lattice-matched or nearly lattice-matched to the substrate. Therefore, the device design is restricted by the lattice parameters of commercially available III-V substrates. For example, in the case of GaSb based type I lasers, the content of As in InGaAsSb quantum wells must be high enough to satisfy the conditions of pseudomorphic growth, but high As content in quantum wells severely affects the device performance [1]. In principle, the problem can be addressed by the epitaxial growth of lattice-mismatched materials of the desired lattice parameters.

The key issue in mismatched epitaxy is to minimize the dislocations that penetrate through the epi-structures. In this work, we expand the lattice parameter of the GaSb substrate by growing linearly compositionally graded Ga(Al)InSb buffers, following the approach in [2-3]. The graded strain in the buffer layers facilitates the glide of threading dislocations and reduces the densities of dislocations that propagate through the buffer layer into the device [2]. High quality $InAs_{1-X}Sb_X$ layers having non-tetragonally distorted, strain-free lattice parameters were grown on top of the buffer layers with thickness up to 1.5 μm.

$InAs_{1-X}Sb_X$ alloys are of special interest, because the bowing effect in the band gap E_g is dependent on the Sb composition, which allows the growth of layers having bandgaps narrower than that in InSb [4-15]. In the second part of the paper, we present the optical properties of non-distorted $InAs_{1-X}Sb_X$ alloys grown on linearly compositionally graded Ga(Al)InSb buffers. Strong PL was observed for $InAs_{1-X}Sb_X$ alloys in a wide temperature range. A relatively long carrier lifetime was obtained in $InAs_{0.8}Sb_{0.2}$ alloys from the PL response to modulated optical excitation.

Growth and Structural Characterization

The heterostructures were grown on GaSb substrates by solid-source molecular beam epitaxy using a Veeco GEN-930 system equipped with As and Sb valved cracker sources. Molecular beam fluxes were measured by an ion gauge positioned in the beam path. The substrate temperature was controlled by a pyrometer, which was calibrated using references such as the III to V enriched surface reconstruction transition, oxide desorption and the melting point of InSb. The compositionally graded 2~3.5 μm thick Ga(Al)InSb buffer layers were grown at temperatures ranging from 460 to 520ºC. The growth temperature was maintained near 415ºC for the InAsSb layers. The Sb incorporation was controlled by the adjustment of the relative pressure of the As and Sb group V elements as measured by the beam-flux-monitor. The growth rate was about 1 μm per hour. $InAs_{1-X}Sb_X$ layers with x = 20, 30 and 44% were grown on GaInSb and AlGaInSb buffers.

The defect distribution in linearly compositionally graded GaInSb and AlGaInSb buffers were characterized by cross-sectional TEM images. Figure 1 shows the XTEM images of structures with either laser or absorber layers grown on top of three different linearly graded buffer layerss;including (a) GaInSb with top In content of 16%; (b) GaInSb with top In content of 30%; (c) AlGaInSb with top Al, Ga and In contents of 75, 0 and 25 %, respectively. The images were taken with a (220) bright field two-beam condition to emphasize the dislocations. In all three structures, the misfit dislocation network was confined in the bottom part (~1.5 μm) of the graded buffers; the topmost portion of the buffers as well as the epi-structures grown onto the buffers is free from misfit dislocations. TEM results did not show any noticeable difference in the dislocation morphology of these two buffer layers or in the laser or absorber layer structures grown on top of them, both appear to be equally efficient in accommodating the misfit strain. From the images, we can estimate that the threading dislocation density is below 10^7 cm^{-2} in the $InAs_{1-X}Sb_X$ layers.

The surface morphology was characterized by atomic force microscopy (AFM) in tapping mode (AFM Dimension V). Cross-hatched patterns with crossing lines along the [110] crystallographic directions were observed on all structures. However, structures grown on AlGaInSb buffers showed better surface morphology. Figure 2 (a) and (b) show the AFM amplitude images measured over a 50 by 50 μm area for samples

Fig. 1. Cross-sectional T
substrates: (a) GaInSb w
content of 30% - mismat
25% - mismatch accomoc

(a)


Fig. 2. AFM amplitude ir
(a) GaInSb buffer and (b)

with $InAs_{0.8}Sb_{0.2}$ lay
undulation amplitude
both nearly twice as
shows the image of
surface roughness, i.
Increasing the Sb co
as indicated by surfa

Strain relaxation
diffraction reciproca
(335) Bragg reflecti
consisting of a 1 μm
AlGaInSb buffer lay
larger than that of Ga
of GaSb to that of A
topmost section of tl

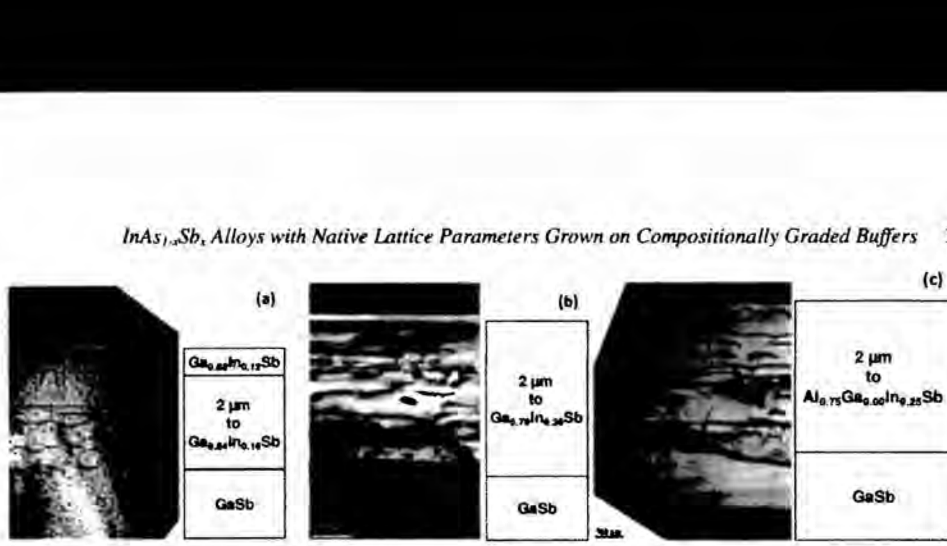

Fig. 1. Cross-sectional TEM images of samples with 2 μm thick linearly graded buffers grown on GaSb substrates: (a) GaInSb with top In content of 16% - mismatch accomodated 0.9%; (b) GaInSb with top In content of 30% - mismatch accomodated 1.4%; (c) AlGaInSb with top Al, Ga and In contents of 75, 0 and 25% - mismatch accomodated 1.4%.

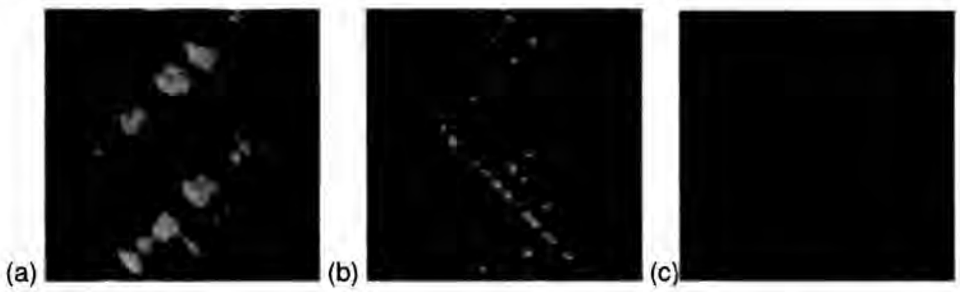

Fig. 2. AFM amplitude images measured over 50 by 50 μm area for samples with $InAs_{0.8}Sb_{0.2}$ layer grown on (a) GaInSb buffer and (b) AlGaInSb buffer; (c) shows the enlarged image (3 by 3 μm) of sample (b).

with $InAs_{0.8}Sb_{0.2}$ layer grown on a (a) GaInSb buffer and a (b) AlGaInSb buffer. The undulation amplitude and period in sample (a) were about 10 nm and 9 μm, respectively, both nearly twice as much the ~ 5nm and ~ 5 μm measured for sample (b). Figure 2 (c) shows the image of sample (b) measured over 3 by 3 μm area; the root mean square surface roughness, i.e., in between of the dips in cross-hatch pattern, was below 1 nm. Increasing the Sb content led to larger peak-to-peak variations in the cross-hatch pattern, as indicated by surface roughness up to 10 nm for the $InAs_{0.56}Sb_{0.44}$ samples.

Strain relaxation of the structures was examined using high-resolution X-ray diffraction reciprocal-space mapping (RSM) at the symmetric (004) and asymmetric (335) Bragg reflections. Figure 3 presents a set of RSM measurements for a structure consisting of a 1 μm $InAs_{0.8}Sb_{0.2}$ layer grown on a 2 μm linearly compositionally graded AlGaInSb buffer layer. The native lattice constant of the $InAs_{0.8}Sb_{0.2}$ layers is about 0.8% larger than that of GaSb. The native lattice constant of the buffer layer changed from that of GaSb to that of $Al_{0.75}Ga_{0.13}In_{0.12}Sb$ with a strain ramp rate about 0.6% per μm. The topmost section of the graded buffer with $Al_{0.75}Ga_{0.13}In_{0.12}Sb$ composition had a native

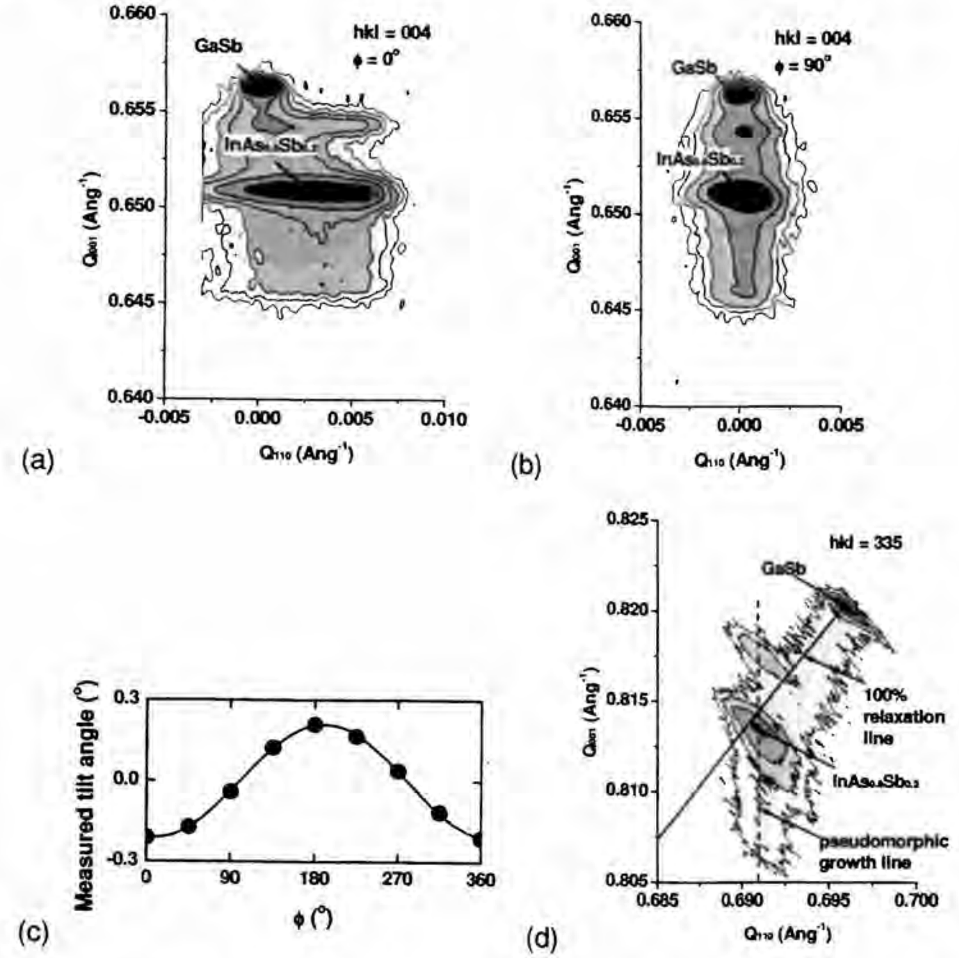

Fig. 3. (a) Symmetric (004) RSM taken at the azimuth angle emphasizing the tilt in the epi-layers; (b) (004) RSM taken at the azimuth angle minimizing the tilt in the epi-layers; (c) dependence of the measured tilt angle as a function of the azimuth angle; (d) asymmetric (335) RSM taken at azimuth angle equal to 90°. Solid line denotes the location of 335 reflexes corresponding to fully relaxed material with lattice parameter gradually increasing from that of GaSb. Dashed line denotes the location of 335 reflexes of the material with further increasing native lattice parameter but grown pseudomorphically to the top of fully relaxed section.

lattice constant about 1.3% larger than that of GaSb, but due to compressive strain, the in-plane lattice constant is equal to the native constant of the bulk $InAs_{0.8}Sb_{0.2}$. When the final structure was grown, the InAsSb layer was sandwiched between $Al_{0.75}Ga_{0.13}In_{0.12}Sb$ carrier confinement layers to assist photoluminescence experiments.

The symmetric reflection revealed the tilt present in the epi-structure. Figure 3 (a) and (b) shows the RSMs obtained near the symmetric (004) reflection at two azimuth angles, namely (a) φ = 0° and (b) φ = 90°, corresponding to two perpendicular [110] crystallographic directions. The tilt angle projected to the measurement plane is

determined from tl
layers. As shown i
bottom part of the
bottom part of the
suggesting that tilti
the projected tilt ar
to be 0.2° in the dir

Asymmetric (3
order to characteri
that the $InAs_{0.8}Sb$
Figure 3 (d) show
i.e., with the minii
the transition from
For illustrative pur
observed relaxatio
relaxed in this sec
and within our ex
topmost section of
the buffer layer is
$InAs_{0.8}Sb_{0.2}$ layer
pseudomorphic se
lattice constant of
below 0.1%; there
InAsSb reflection
strained auxiliary
calibration purpose

Optical Characte

The PL and absor
spectrometer equi
wavelength of 12
laser and collected
temperature range
shows the PL spec
13, 150 and 300 I
$InAs_{0.56}Sb_{0.44}$ laye
InAs/GaSb superla
300 periods of InA
AlAsSb carrier co
width at half max
intensities from b

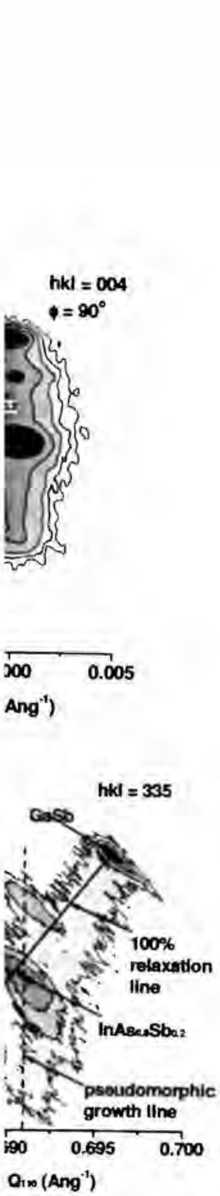

ı the epi-layers; (b) (004) of the measured tilt angle le equal to 90°. Solid line ıttice parameter gradually the material with further ıxed section.

npressive strain, the $As_{0.8}Sb_{0.2}$. When the n $Al_{0.75}Ga_{0.13}In_{0.12}Sb$

ucture. Figure 3 (a) tion at two azimuth perpendicular [110] ısurement plane is

determined from the horizontal peak separation between the GaSb substrate and the epi-layers. As shown in Figure 3 (a), the tilt angle increases as the thickness increases in the bottom part of the graded buffer, and stops increasing in the consequent layers. The bottom part of the buffer layers is near completely relaxed, as will be shown later, suggesting that tilting is associated with the process of strain relaxation. Figure 3 (c) plots the projected tilt angle as a function of several azimuth angle φ. We estimate the tilt angle to be 0.2° in the direction about 10° away from the [110] direction (φ = 90°).

Asymmetric (335) RSM reflexes were measured at four different azimuth angles in order to characterize the degree of relaxation of the graded buffer layer and to confirm that the $InAs_{0.8}Sb_{0.2}$layer is lattice-matched to the topmost part of the graded buffer. Figure 3 (d) shows one of the (335) RSMs measured at an azimuth angle equal to 90°, i.e., with the minimum tilting effect. The shift visible in the (335) RSM corresponds to the transition from the strain relaxed to the pseudomorphic section of the graded buffer. For illustrative purposes, the solid line corresponds to a 100% relaxed square lattice. The observed relaxation is close to 100%. After the tilt angle is accounted for, the degree of relaxed in this section of the graded buffer can be estimated as 95%, i.e., nearly 100%, and within our experimental error. The pseudomorphic growth of the dislocation-free topmost section of the buffer layer is apparent from the (335) scan since the reflex from the buffer layer is nearly vertical (dashed line in Figure 3 (d)). The reflection from the $InAs_{0.8}Sb_{0.2}$ layer is located at the turning point and on the same vertical line as the pseudomorphic section of the buffer, which confirms lattice matching to the in-plane lattice constant of the graded buffer layer. The amount of strain in the $InAs_{0.8}Sb_{0.2}$ layer is below 0.1%; therefore, no strain relaxation is expected. The reflection located above the InAsSb reflection in both the (004) and (335) RSM corresponds to a pseudomorphically strained auxiliary AlGaSb layer (~150 nm) that was grown on top of the InAsSb layer for calibration purposes.

Optical Characterization

The PL and absorption spectra were measured with a Fourier-transform infrared (FTIR) spectrometer equipped with a liquid-nitrogen cooled HgCdTe detector with a cut-off wavelength of 12 μm. The PL was excited by either a 970 nm laser diode or a Nd:YAG laser and collected by reflective optics. PL was observed from all structures in a wide temperature range, up to room temperature from samples with 20% Sb. Figure 4 (a) shows the PL spectra from 1-μm thick $InAs_{0.8}Sb_{0.2}$ layer grown on an AlGaInSb buffer at 13, 150 and 300 K. Figure 4 (b) presents the PL spectra measured from a 1-μm thick $InAs_{0.56}Sb_{0.44}$ layer grown on an AlGaInSb buffer and a 1.8-μm thick long-wave InAs/GaSb superlattice grown on a GaSb substrate. The superlattice structure consists of 300 periods of InAs and GaSb layers with the cell period of 63 Å enclosed within 20-nm AlAsSb carrier confinement layers lattice-matched to GaSb. The spectral widths (full-width at half maximum) for the three samples were similar, about 11 meV. The PL intensities from both $InAs_{0.56}Sb_{0.44}$ and superlattices were comparable at 13 K while

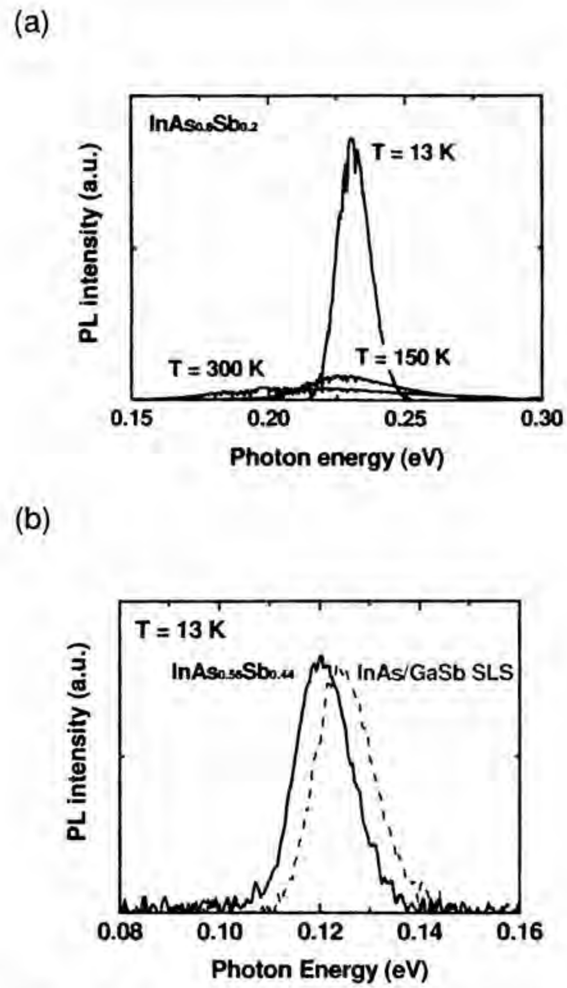

Fig. 4. (a) PL spectra from $InAs_{0.8}Sb_{0.2}$ sample grown on AlGaInSb buffer at 13 K, 150 K and 300 K under an excitation power of 0.5W. (b) PL spectra from $InAs_{0.56}Sb_{0.44}$ layer grown on AlGaInSb buffer and long-wave InAs/GaSb superlattices grown on GaSb substrate at 13 K under an excitation of 0.1 W. The PL was excitation by a Nd:YAG laser with a beam diametc: of about 0.5 mm.

intensities drops much faster in InAsSb sample at elevated temperatures. Considering the challenge of creating adequate hole confinement in the As-rich alloys, the faster drop of the PL intensity with temperature can be explained by the increased diffusion of the excess carriers out of the InAsSb layer.

The absorption spectra were measured for the InAsSb layers with Sb compositions of 20% and 30% grown on GaInSb buffers. The absorbance was determined from transmission measurements taking into account the multiple reflections. The absorption spectrum was derived by subtracting the absorbance of the heterostructure with the epi-layers and the substrate. The transmission of the substrate was determined using the

same sample after th
with 20% Sb was th
was lapped down to
GaSb at longer wav
the GaSb substrates
thickness of 55 μm
transmission for th
substrate was detern
substrate. Both abs
presented in Figure
the PL was associate

Fig. 5. Absorption and l
excited by a 970-nm lase
near 0.29 eV was caused

same sample after the epi-layers were removed by polishing. The substrate of the sample with 20% Sb was thinned to 300 µm. The substrate of the heterostructure with 30% Sb was lapped down to near 50 µm thickness because of high free carrier absorption in the GaSb at longer wavelengths. The latter was determined to be 140 cm^{-1} near $\lambda = 8$ μm for the GaSb substrates with Te doping level of 3×10^{18} cm^{-3}. The sample with the measured thickness of 55 µm had near 50% transmission at this wavelength, as compared to a 2% transmission for the 300 µm-thick substrate. The free carrier absorption in the thin substrate was determined by a fit based on the absorption measurements for the thicker substrate. Both absorption and PL spectra measured for the two samples at 150 K are presented in Figure 5. The PL peak energy matched the absorption edge indicating that the PL was associated with the band-to-band recombination.

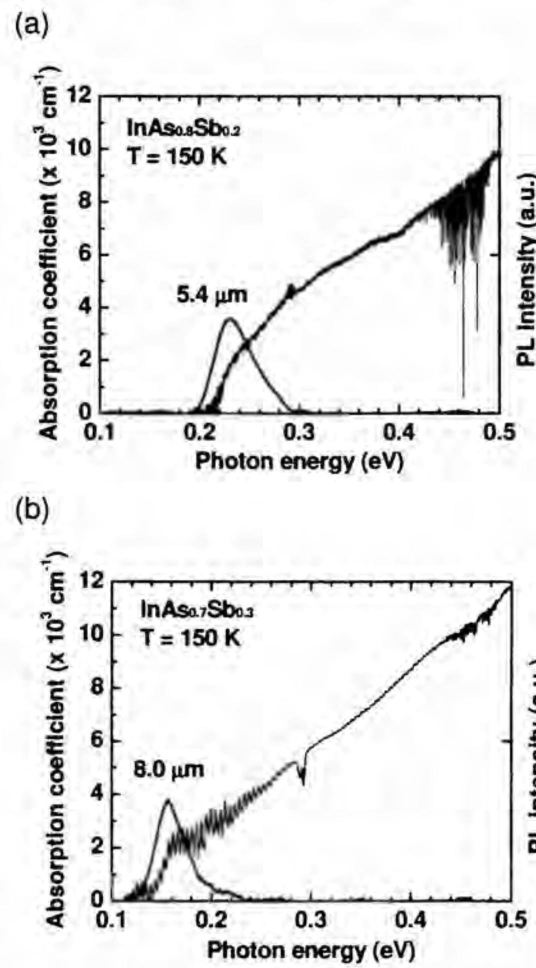

Fig. 5. Absorption and PL spectra measured at 150 K for (a) $InAs_{0.8}Sb_{0.2}$ and (b) $InAs_{0.7}Sb_{0.3}$. The PL was excited by a 970-nm laser diode at a power of 400 mW; the excitation area was 2.5×10^{-3} cm^2. The distortion near 0.29 eV was caused by CO2 absorption.

The energy positions of PL maxima at T = 13 K versus Sb composition x in the InAsSb layers are presented in Figure 6. The positions of PL maxima were used to determine the bandgaps and the bowing parameter, which was about 0.9 eV, considerably greater than the recommended value of 0.7 eV [15]. The lower value of bowing reported previously was based on measurements in materials grown without control of the strain relaxation. The observed difference in the bowing between the 0.9 eV determined in this work and the 0.7 eV reported in literature can be explained by the absence of residual strain in the InAsSb epitaxial layers.

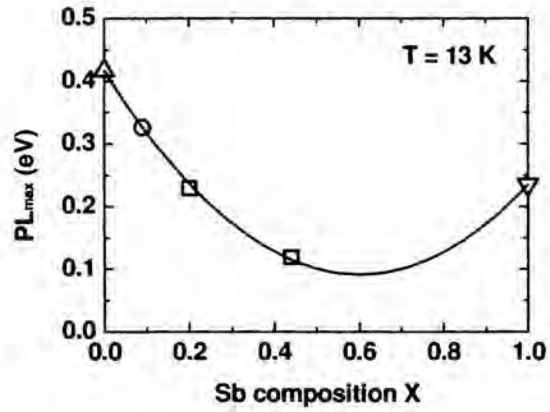

Fig. 6. Dependence of 13K PL maxima on composition X in InAs1-XSbX epitaxial layers: InAs epilayer grown on InAs substrate (triangle), InAsSb0.08 epilayer grown lattice matched to GaSb substrate (circle), InAs1-XSbX epilayers grown on AlGaInSb buffers (squares) on GaSb substrate, InSb epilayers grown on InSb substrate (inverted triangles).

Carrier lifetime measurements for the 1-μm thick $InAs_{0.8}Sb_{0.2}$ layer grown on AlGaInSb buffer layer were performed at T = 77 K using optical modulation response technique [16]. To minimize the effects of carrier separation on the carrier lifetime in undoped InAsSb layers, the Al0.25Ga0.70In0.05Sb barriers were doped with Be to the level of 1×10^{17} cm^{-3}. The dependence of the carrier lifetime on the excitation power is shown in Figure 7. Simulation of the band diagram showed that the minority holes remain confined under low excitation (inset of Figure 7 (b)). The carrier lifetime was determined from the PL response to a small signal modulation of excitation in the frequency domain. The PL response spectra in a range of continuous-wave excitation power are shown in Figure 7 (a). The carrier lifetime τ corresponding to the cut-off frequency (-3dB point) was obtained by fitting the response in the entire frequency range to the dependence $PL_\omega \propto [1 + (2\pi f \times \tau^2)^2]^{-1/2}$. A 250 ns carrier lifetime under low excitation condition was measured. The excess carrier concentration was estimated to be in the range $(2\text{-}4)\times10^{15}$ cm^{-3} at the excitation power in the range of 0.5-1 W/cm^2.

Fig. 7. Carrier lifeti
buffer on a GaSb su
levels of 0.8, 1, 1.4,
1.31 μm, and the exc
continuous-wave ex
used for carrier lifeti

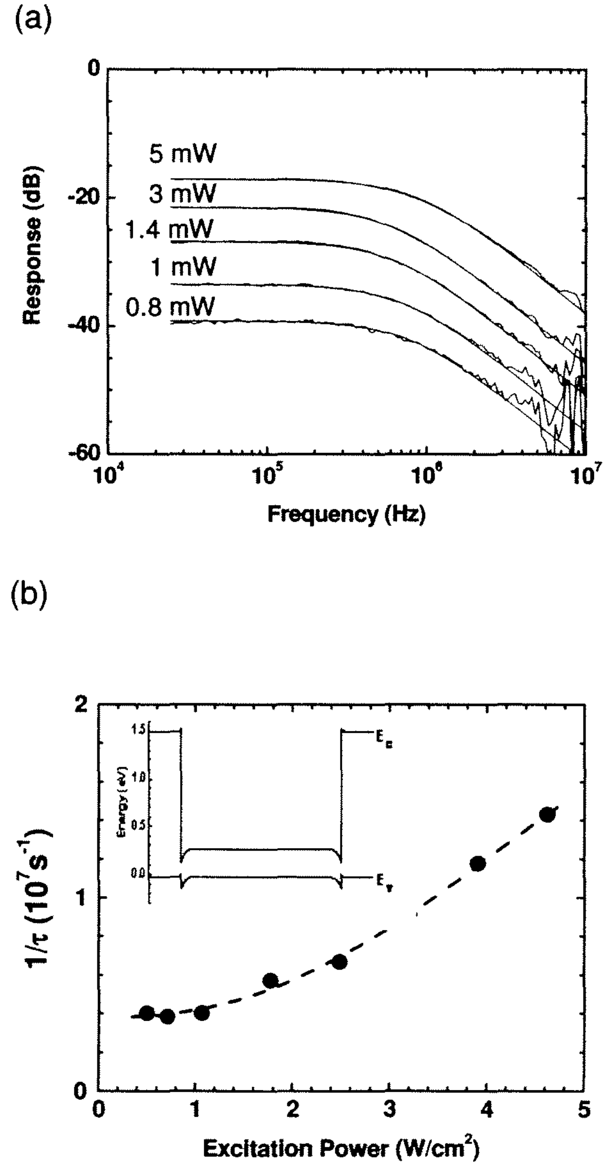

Fig. 7. Carrier lifetime measurements at T= 77 K on a 1-μm-thick $InAs_{0.8}Sb_{0.2}$ layer grown on an AlGaInSb buffer on a GaSb substrate. The PL responses and fits are presented for continuous wave excitation power levels of 0.8, 1, 1.4, 3 and 5 mW from bottom to top, respectively. The PL was excited at the wavelength of 1.31 μm, and the excitation area was 2×10^{-3} cm^2 FWHM (left). The reciprocal carrier lifetime is plotted versus continuous–wave excitation power density (right). A schematic band diagram of the InAsSb heterostructure used for carrier lifetime measurements is shown in the inset.

Conclusion

In summary, we conclude that growing compositionally graded buffers (Ga(Al)InSb on GaSb substrates) with a strained but unrelaxed top layer allows the fabrication of bulk $InAs_{1-x}Sb_x$ layers (0.5~1.5 μm thick). These films have characteristics that are promising for the development of IR detectors operating within the spectral range from 5 to 12 μm. The critical element of the technology is the control of the in-plane lattice constant of the topmost section of the buffer. The in-plane lattice constant of this layer must be equal to the lattice constant of $InAs_{1-x}Sb_x$ with given x. The unrelaxed $InAs_{1-x}Sb_x$ epitaxial layers grown on top of such buffers demonstrated photoluminescence in the spectral range from 5.2 to 9.4 μm within the temperature range of 77~150 K. The carrier lifetime of 250 ns was obtained at T = 77 K for structure consisting $InAs_{0.8}Sb_{0.2}$ epi-layers.

Acknowledgement

This work was supported by the National Science Foundation, Grant DMR0710154 and Army Research Office, Grant W911NF11-1-0109. The authors would like to thank IQE, Inc. for providing the superlattice samples.

References

[1] L. Shterengas, G. L. Belenky, J. G. Kim and R. U. Martinelli, *Semicond. Sci. Tech.* **19**, 655 (2004).
[2] J. Tersoff, *Appl. Phys. Lett.* **62**, 693 (1993).
[3] G. Kipshidze, T. Hosoda, W. L. Sarney, L. Shterengas, and G. Belenky, *IEEE Photon. Technol. Lett.* **23**, 317 (2011).
[4] Z. M. Fang, K. Y. Ma, D. H. Jaw, R. M. Cohen, and G. B. Stringfellow, *J. Appl. Phys.* **67**, 7034 (1990).
[5] G. S. Lee, Y. Lo, Y. F. Lin, S. M. Bedair, and W. D. Laidig, *Appl. Phys. Lett.* **47**, 1219 (1985).
[6] Y. B. Li, S. S. Dosanjh, I. T. Ferguson, A. G. Norman, A. G. de Oliveira, R. A. Stradling, and R. Zallen, *Semicond. Sci. Technol.* **7**, 567 (1992).
[7] M. Y. Yen, R. People, and K. W. Wecht, *J. Appl. Phys.* **64**, 952 (1988).
[8] C. G. Bethea, B. F. Levine, M. Y. Yen, and A. Y. Cho, *Appl. Phys. Lett.* **53**, 291 (1988).
[9] J. D. Kim, D. Wu, J. Wojkowski, J. Poitrovski, J. Xu, and M. Razeghi, *Appl. Phys. Lett.* **68**, 99 (1996).
[10] S. R. Kurtz, L. R. Dawson, R. M. Biefeld, D. M. Follstaedt, and B. L. Doyle, *Phys. Rev. B* **46**, 1909 (1992).
[11] T.-Y. Seong, G. R. Booker, A. G. Norman, and I. T. Ferguson, *Appl. Phys. Lett.* **64**, 3593 (1994).
[12] S. Nakamura, P. Jayavel, Y. Kobayashi, K. Arafune, T. Koyama, M. Kumagawa, and Y. Hayakawa, *Semicond. Sci. Technol.* **20**, 1064 (2005).
[13] G. Belenky, D. Denetsky, G. Kipshidze, D. Wang, L. Shterengas, W. L. Sarney and S. P. Svensson, *Appl. Phys.Lett.* **99**, 141116 (2011).
[14] G. Belenky, G. Kipshidze, D. Donetsky, S.P. Svensson, W.L. Sarney, H. Hier, L. Shterengas, D. Wang, and Y. Lin, *Proc. SPIE* 8012, 80120W (2011).
[15] I. Vurgaftman, J. R. Meyer and L. R. Ram-Mohan, *J. Appl. Phys.* **89**, 5815 (2001).
[16] D. Donetsky, S. P. Svensson, L. E. Vorobjev, and G. Belenky, *Appl. Phys. Lett.* **95**, 212104 (2009).